Apprentissage de variétés pour la mécanique des matériaux

David Ryckelynck,

Daria Mesbah, Simon Le Berre, Axel Aublet, Hamza Boukraichi, Pablo Alvarez Pereira, Hugo Launay, Thomas Daniel, Youssef Hammadi, Harris Farooq, Laurent Lacourt, William Hilth, Jules Fauque, Tuan Dinh Trong, Clément Olivier, Yang Zhang, Samuel Jules, Mélanie Leroy, Bahram Sarbandi, Sophie Cartel, Florence Vincent, Laurent Vanoverberghe, Djamel Missoum Benziane

Chair BigMéca Safran-MINES Paris,
PSL research university, Centre des Matériaux, France

GdR Géométrie Différentielle et Mécanique - Paris, Novembre 2022

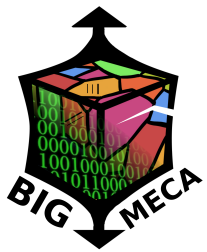

What is machine learning ?

Machine Learning is a subfield of Artificial Intelligence. ML algorithms make computers behave more "intelligently" by generalizing rather than merely storing and retrieving data (like a database system would do).

The learning task (training task) is performed on a train set of data by solving an optimization problem (a minimization of a loss function).

Generalization capabilities are evaluated on a test set of data, that contains unseen data during the training.

Avancée importante en 2012 : Deep learning in computer vision

Convolutional neural networks [Le Cun 1989], using "large" number of layers and "large" number units, were some of the first deep models to perform well in 2012 as classifiers [Krizhevsky et al. 2012] (10^4 categories in 10^7 images) [a].

ImageNet

a. Krizhevsky, A. Sutskever, I. and Hinton, G. (2012). ImageNet classification with deep convolutional neural networks. In NIPS'2012.

Remarks : No parameter for the content of images. Images are structured data having a tensor shape. Some simulated data too...

Contents

Data in model-based engineering

In various fields, a parametric modeling is available ($\mu \in \mathcal{P}$) on informatics platforms :

- Aeronautics industry
- Automotive industry
- Rail industry
- Shipbuilding industry
- Energy industry
- Manufacturing industry
- Medical Equipment
- ...

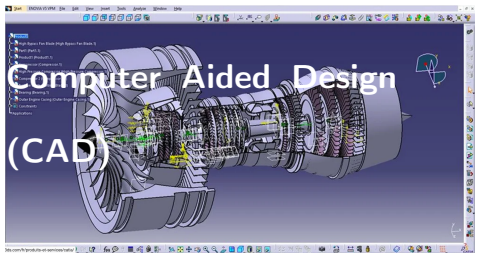

$\mu_\square$: digital images

(huge ambient space)

X-Ray Diffraction Tomography [Proudhon 2014]

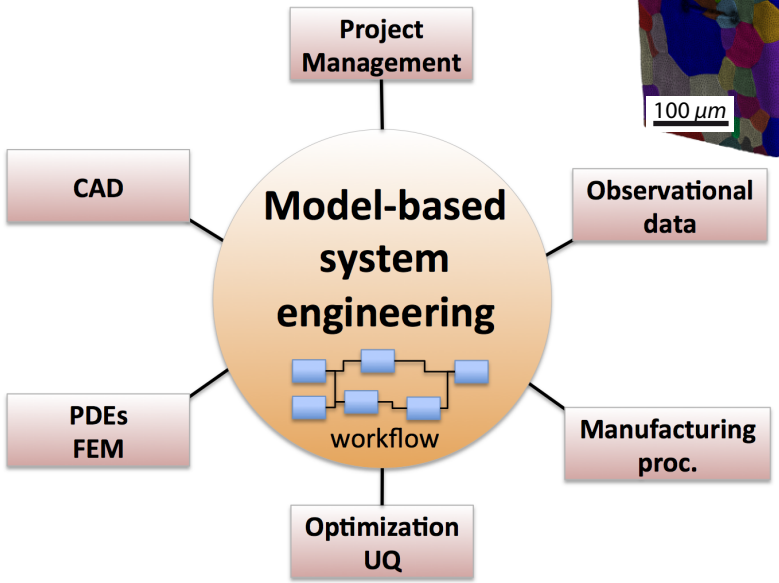

Parametric predictions

$\mathbf{u}(\mathbf{x}, t, \boldsymbol{\mu}, \boldsymbol{\mu}_\square)$

Data in model-based engineering

In various fields, a parametric modeling is available ($\mu \in \mathcal{P}$) on informatics platforms :

- Aeronautics industry
- Automotive industry
- Rail industry
- Shipbuilding industry
- Energy industry
- Manufacturing industry
- Medical Equipment
- ...

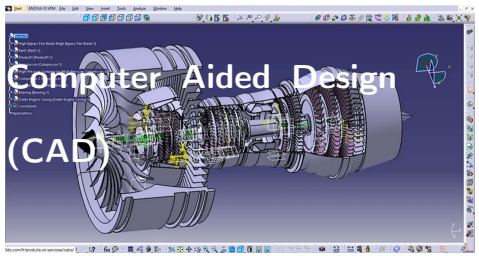

$\mu_\square$: digital images

(huge ambient space)

X-Ray Diffraction Tomography [Proudhon 2014]

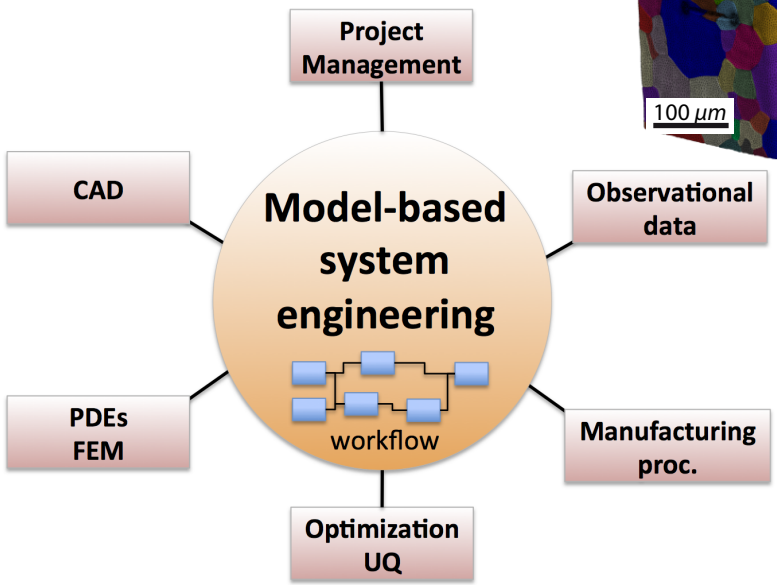

Parametric predictions

$\mathbf{u}(\mathbf{x}, t, \boldsymbol{\mu}, \boldsymbol{\mu}_\square)$

Images reveal many uncer-tainties!

Domaine de validité des modèles issus de jumeaux numériques

E = espace de validité de modèles éléments finis réduits

Contents

Examples of data sets at Centre des Matériaux

- Hyper-reduced direct numerical simulation of voids in welded joints via image-based modeling (Laurent Lacourt's PhD CEA)
- Mechanical Fatigue Testing Under Thermal Gradient and Manufacturing Variabilities in Nickel-Based Superalloy Parts with Air-Cooling Holes (Axel Aublet's PhD Safran).
- Model order reduction assisted by deep neural networks (ROM-net) (Thomas Daniel's PhD Safran)

Numerical simulation of voids in welded joints via image-based modeling - CEA (L. Lacourt's PhD)

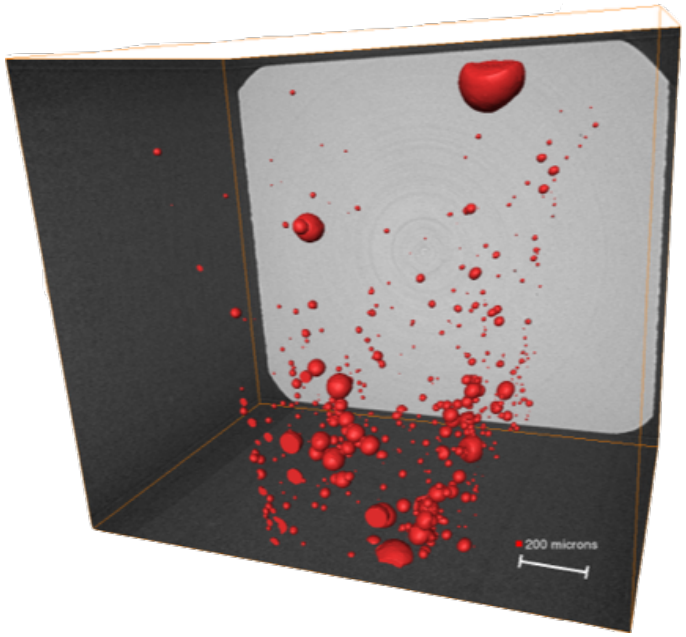

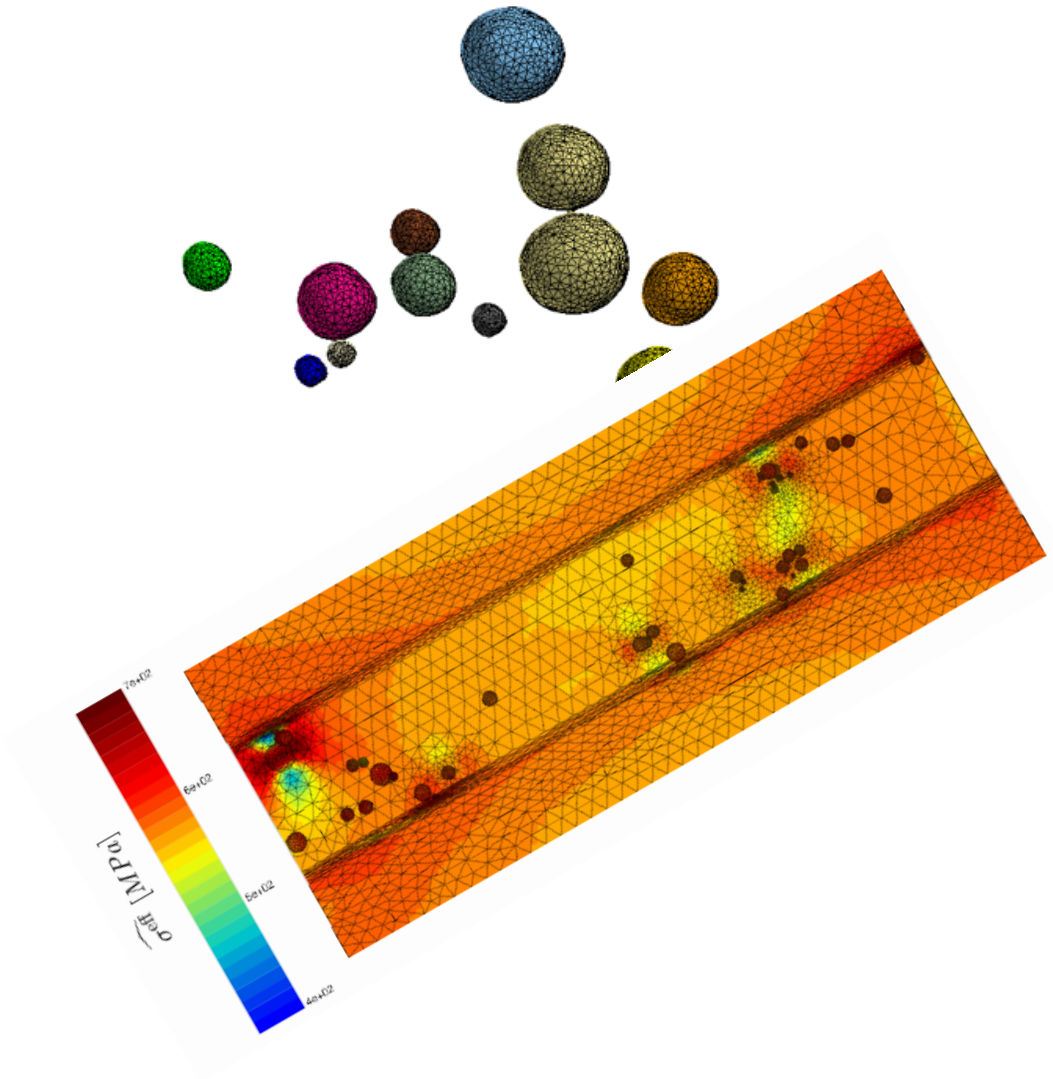

Numerical simulation of voids in welded joints v… image-based modeling - CEA (L. Lacourt's PhD)

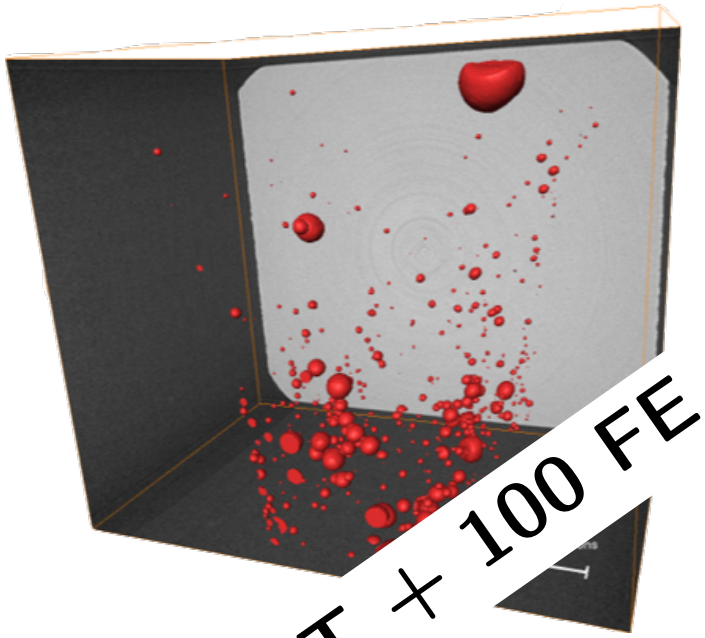

1 X-Ray CT + 100 FE simulations+4000 submodels

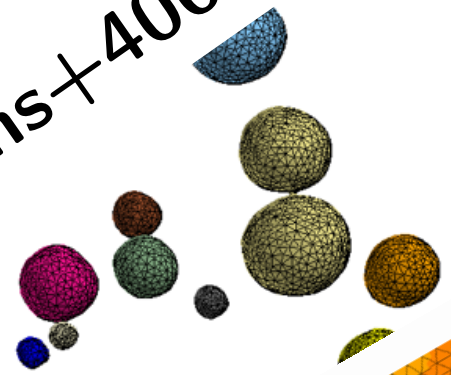

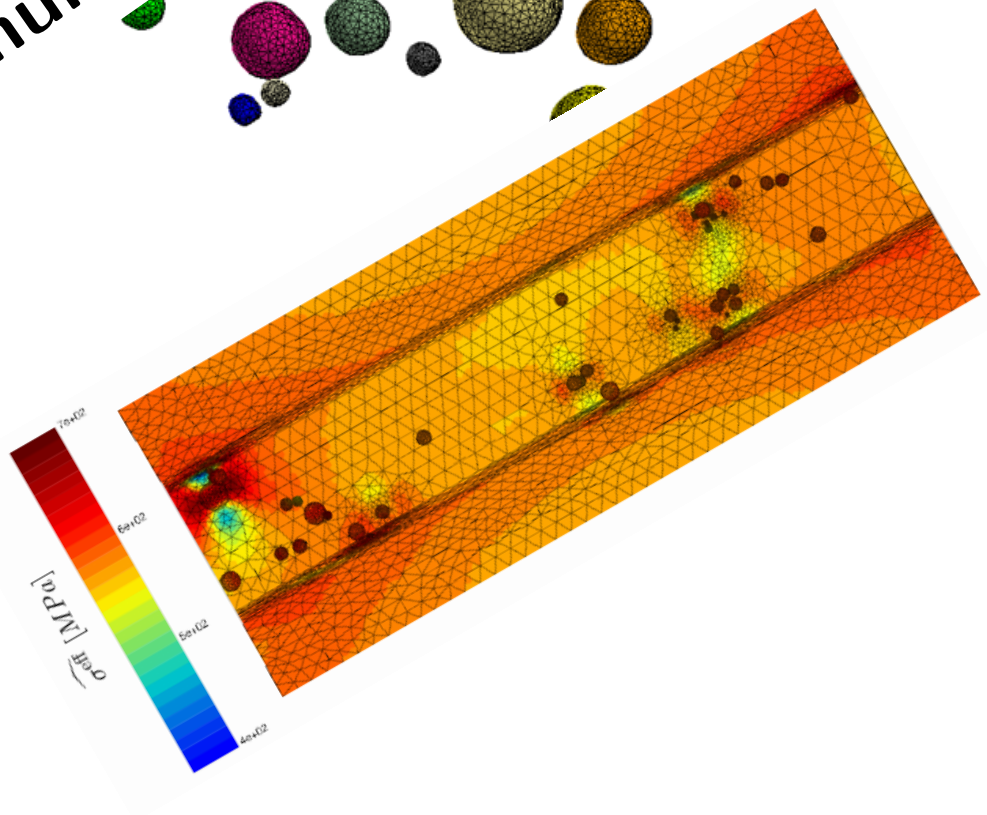

Mechanical Fatigue Testing Under Thermal Gradient and Manufacturing Variabilities in Nickel-Based Superalloy Parts - Safran (A. Aublet's PhD)

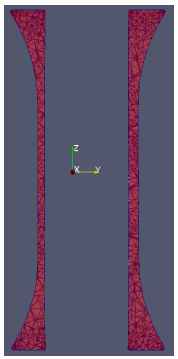

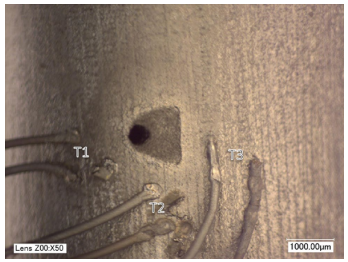

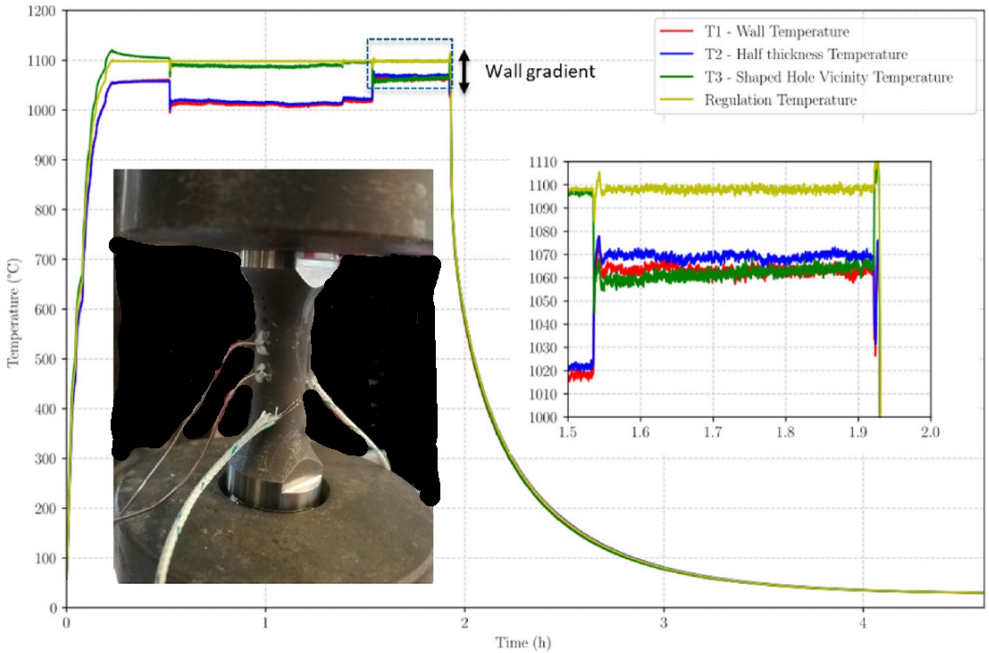

Mechanical Fatigue Testing Under Thermal Gradien[illegible] Manufacturing Variabilities in Nickel-Based Su[illegible]oy Parts - Safran (A. Aublet's PhD)

40 X-Ray CT + 40 Digital Twins + 4000 FE Submodels

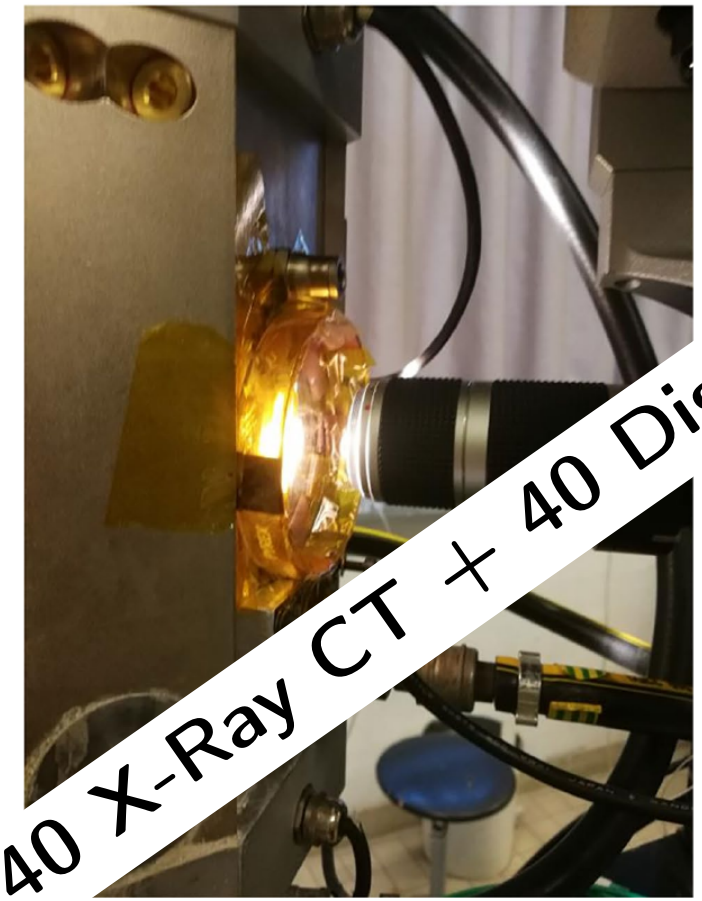

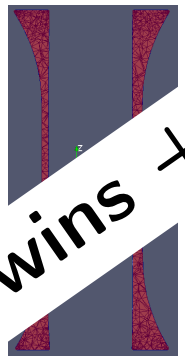

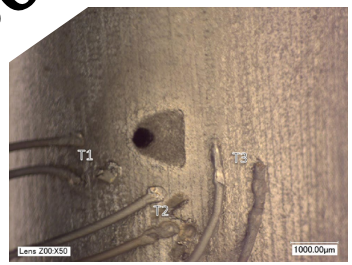

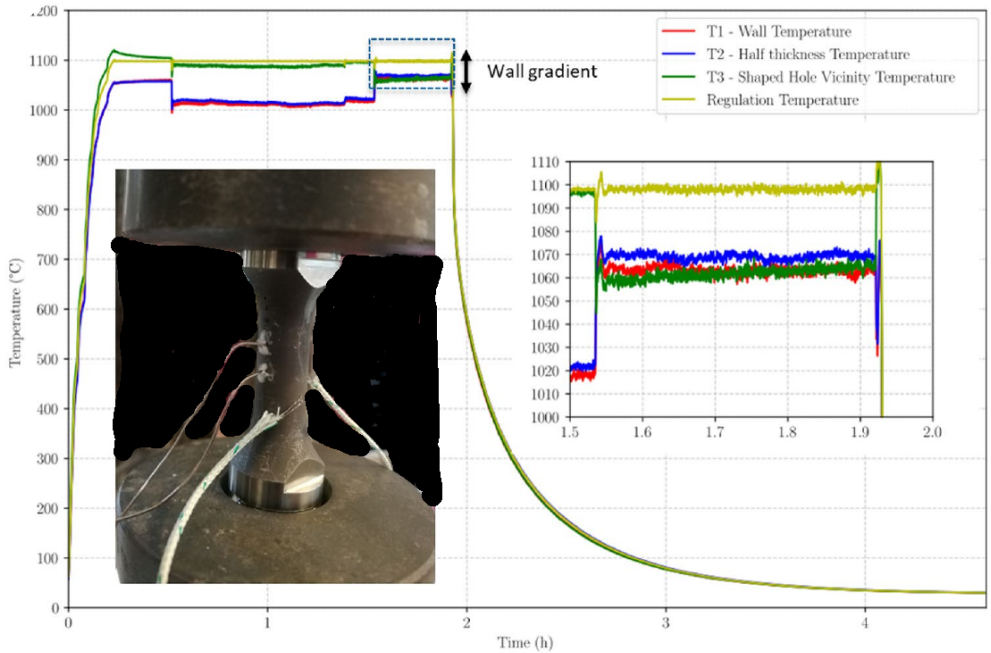

Stochastic thermomechanical predictions for lifetime estimation - Safran (Th. Daniel PhD)[1]

Input data **d** : stochastic temperature field (as a 3D tensor of data).

Output **u** : stress and plastic fields.

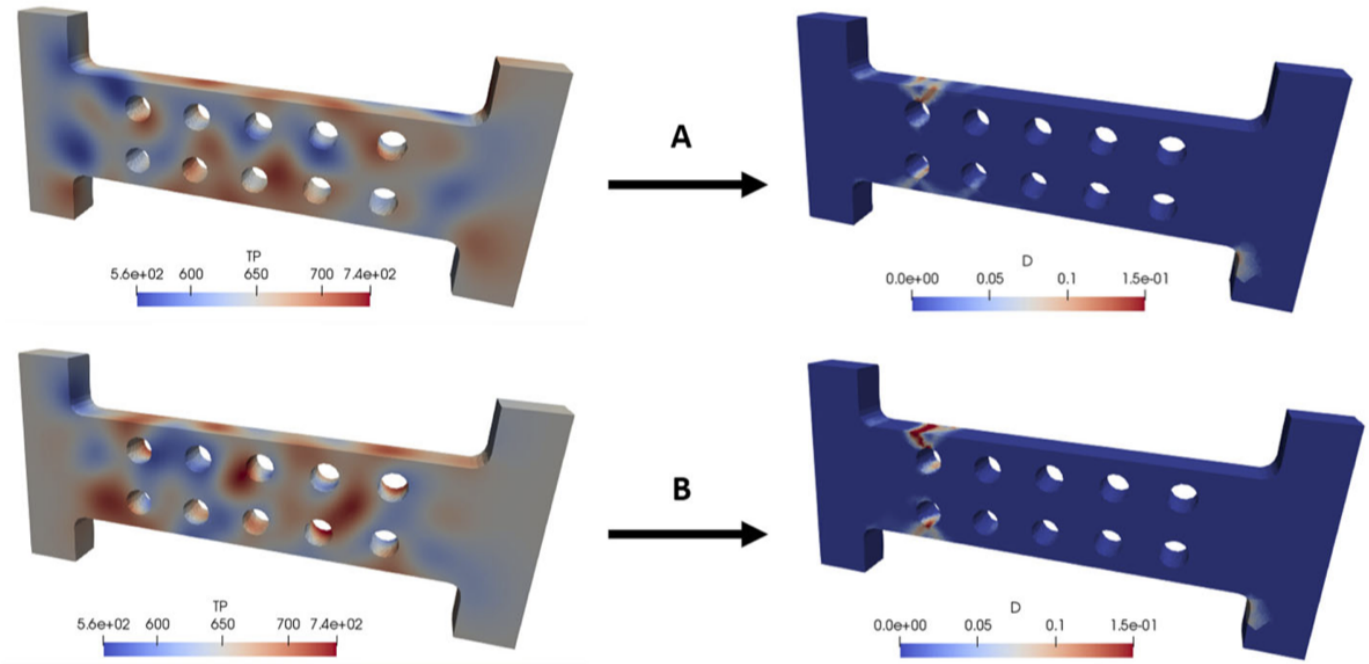

Fig. 6 Influence of the temperature field. Two damage fields (on the right) obtained from two different temperature fields (on the left)

1. Thomas Daniel, Fabien Casenave, Nissrine Akkari, David Ryckelynck. Model order reduction assisted by deep neural networks (ROM-net). Advanced Modeling and Simulation in Engineering Sciences, SpringerOpen, 2020, 7 (1), doi :10.1186/s40323-020-00153-6

Stochastic thermomechanical predictions for lifetime estimation - Safran (Th. Daniel PhD)[1]

Input data **d** : stochastic temperature field (as a 3D tensor of data).

Output **u** : stress and plastic fields.

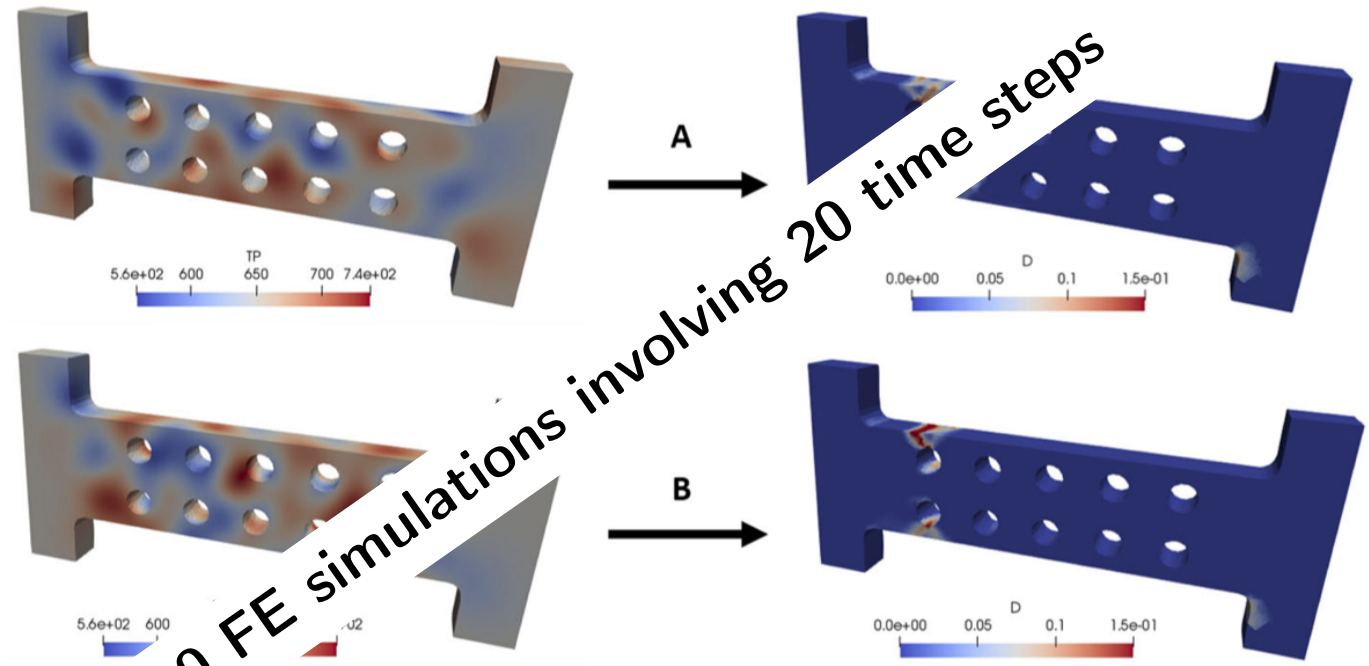

Fig. 6 ...ce of the temperature field. Two damage fields (on the right) obtained from two different temperat...e fields (on the left)

1. Thomas Daniel, Fabien Casenave, Nissrine Akkari, David Ryckelynck. Model order reduction assisted by deep neural networks (ROM-net). Advanced Modeling and Simulation in Engineering Sciences, SpringerOpen, 2020, 7 (1), doi :10.1186/s40323-020-00153-6

Image-based models have no parametric modeling

Setting a parameter space for image-base modeling is, most of the time, a huge simplification of the details contained in high-resolution digital images !
But mechanics of materials is in the details.

Today, image-based meshes are the common rule for image-based modeling.

Digital twin = a real instance of a mechanical component + PDEs coupled to observational data + approximation space + ... [2]

2. Glaessgen, E. and Stargel, D. (2012). The digital twin paradigm for future nasa and u.s. air force vehicles. In Structures, Structural Dynamics, and Materials Conference (Aerospace Research Central). doi :10.2514/6.2012-1818

Learning vector-bundle manifolds (fibré vectoriel)

Our ultimate goal is to create a vector bundle : a family of vector subspaces parametrized by points on a base manifold ($\mathcal{B}$). Here the total space E is a manifold that contains : Mechanical predictions for both digital twins on $\mathcal{B}$ and "similar" mechanical states.

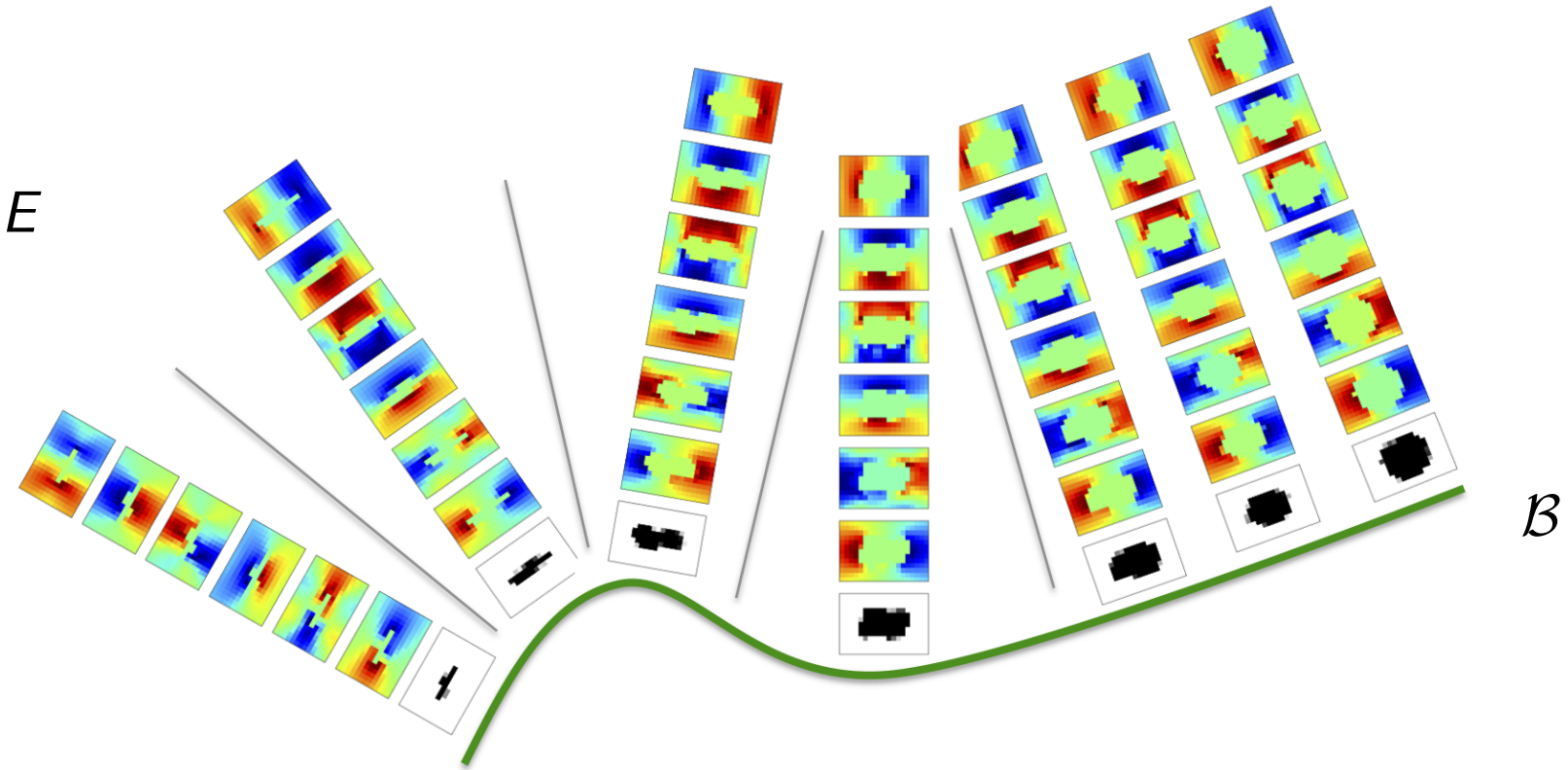

$$\mathbf{u}(\cdot;\boldsymbol{\mu}_{\square}) \in \mathcal{B}, \quad \mathbf{u} \in \mathcal{B} \rightarrow \text{span}(\mathbf{V}(\mathbf{u})) \in \text{Gr}(N,\mathcal{N}), \quad \mathbf{V}(\mathbf{u})^T\,\mathbf{V}(\mathbf{u}) = \mathbf{I}$$

Learning vector-bundle manifolds : motivation

For each digital twin, we have setup a high fidelity model. The predictions of this high fidelity model belongs to a Base manifold $\mathcal{B}$ and a vector subspace. The related reduced order model has a validity domain that is not restricted to the instance of digital twin.

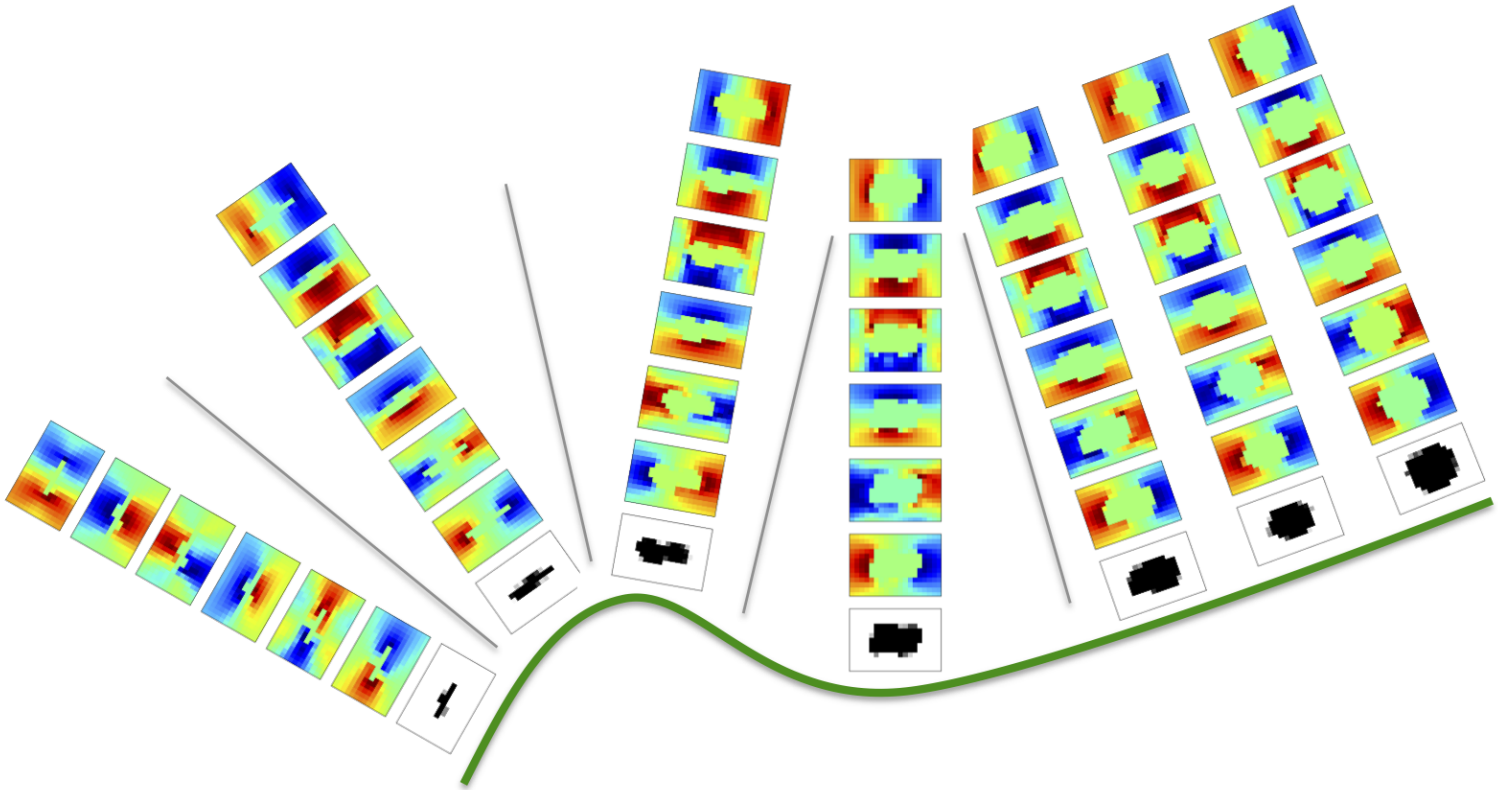

Contents

Ellipticity

Linear elasticity follows elliptic equations :

$$\partial\Omega = \partial_D\Omega \cup \partial_N\Omega \quad \partial_D\Omega \cap \partial_N\Omega = \emptyset$$

$$\text{div}\boldsymbol{\sigma} = 0 \quad \forall \mathbf{x} \in \Omega, \qquad \boldsymbol{\sigma} \cdot \mathbf{n} = F \quad \mathbf{x} \in \partial_N\Omega$$

$$\boldsymbol{\sigma} = \mathbf{C} : \varepsilon^e \quad \forall \mathbf{x} \in \Omega$$

$$\varepsilon^e = \frac{1}{2}\left(\nabla \mathbf{u} + \nabla \mathbf{u}^T\right) \quad \forall \mathbf{x} \in \Omega, \qquad \mathbf{u} \in \mathcal{V}$$

$$\mathcal{V} = \left\{\mathbf{v} \in H^1(\Omega)\,,\, \mathbf{v} = \mathbf{u}_D \quad \mathbf{x} \in \partial_D\Omega\right\} \quad \text{Hilbert space}$$

Céa's lemma for elliptic partial differential equations ($\mathbf{u}_D = 0$)

Céa's Lemma about approximation spaces : Let's $\mathcal{V}_\mathcal{N}$ be a vector subspace of dimension $\mathcal{N}$, $\mathcal{V}_\mathcal{N} \subset \mathcal{V}$, let's denote by $\mathbf{v}_\mathcal{N}$ the closest approximation of $\mathbf{u}$ in $\mathcal{V}_\mathcal{N}$, let's denote by $\mathbf{u}_\mathcal{N}$ the solution of the Galerkin projection of the elliptic equations in the approximation space $\mathcal{V}_\mathcal{N}$. It exists $c > 0$ such that,

$$\|\mathbf{u} - \mathbf{u}_\mathcal{N}\|_{L^2(\Omega)} \leq c \inf_{\mathbf{v}_\mathcal{N} \in \mathcal{V}_\mathcal{N}} \|\mathbf{u} - \mathbf{v}_\mathcal{N}\|_{L^2(\Omega)}$$

The closer $\mathbf{u}$ to the approximation space $\mathcal{V}_\mathcal{N}$, the better its prediction $\mathbf{u}_\mathcal{N} \in \mathcal{V}_\mathcal{N}$.

Model order reduction using a Galerkin projection :

- Let's $\mathcal{V}_N \subset \mathcal{V}_\mathcal{N}$ be a reduced approximation space for $\mathcal{V}_\mathcal{N}$ ($N \ll \mathcal{N}$).
- The closer $\mathbf{u}$ to the reduced approximation space $\mathcal{V}_N$, the better its prediction $\mathbf{u}_N \in \mathcal{V}_N$.
- Manifold learning for $\mathbf{u}$ is very appealing !

Here the solution space is the singleton $\{\mathbf{u}\}$. The approximation space is expected to be larger than the solution space, hence it is supplemented by a set of equations.

Ellipticity in generalized standard plasticity

$$\partial\Omega = \partial_D\Omega \cup \partial_N\Omega \quad \partial_D\Omega \cap \partial_N\Omega = \emptyset$$

$$\mathrm{div}\boldsymbol{\sigma} = 0 \quad \forall \mathbf{x} \in \Omega, \qquad \boldsymbol{\sigma} \cdot \mathbf{n} = F \quad \mathbf{x} \in \partial_N\Omega$$

$$\boldsymbol{\sigma} = \mathbf{C} : \varepsilon^e \quad \forall \mathbf{x} \in \Omega$$

$$\varepsilon = \frac{1}{2}\left(\nabla\mathbf{u} + \nabla\mathbf{u}^T\right), \quad \varepsilon = \varepsilon^e + \varepsilon^p \quad \forall \mathbf{x} \in \Omega, \qquad \mathbf{u} \in \mathcal{V}$$

$$\mathcal{V} = \left\{\mathbf{v} \in H^1(\Omega)\,,\, \mathbf{v} = \mathbf{u}_D \quad \mathbf{x} \in \partial_D\Omega\right\} \quad \text{Hilbert space}$$

Incremental standard plasticity is approximated by a series of elliptical predictions $\Delta\mathbf{u}^{(i)}$:

$$\dot{\mathbf{u}}\, dt \approx \sum_i \Delta\mathbf{u}^{(i)}$$

$$\boldsymbol{\sigma} = \frac{\partial w_\Delta}{\partial \varepsilon}(\varepsilon(\mathbf{u}); \ldots) \ \ldots$$

where w_Δ is a convex incremental potential [Miehe 2002].

Contents

Machine learning applied to synthetic data forecast by physics-based models

We collect each mechanical predictions, time step after time step, during numerical simulations of plasticity : $\mathbf{u}(\mathbf{x}, t_j, \mu_k, \mu_{\square p}) \in \mathcal{V}_{\mathcal{N}}$

Parameter set for the train set : $\mathcal{D} = \{(t_1, \mu_1, \mu_{\square 1}), \ldots, (t_j, \mu_k, \mu_{\square p})\}$

A posteriori model reduction

XXL dof

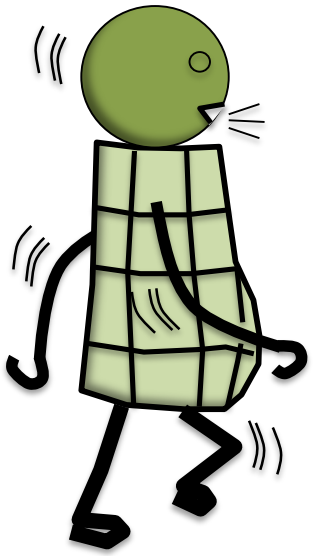

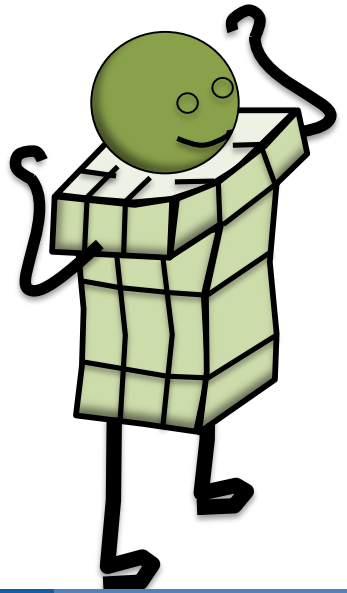

Manifold learning for $\mathcal{V}_N \subset \mathcal{V}_\mathcal{N}$

The ambient space is designed, a priori, to collect the data. Usually, the data occupy a latent space that does not fill the entire ambient space.

Manifold learning aims to find a data representation that retains the main information hidden in a train set.

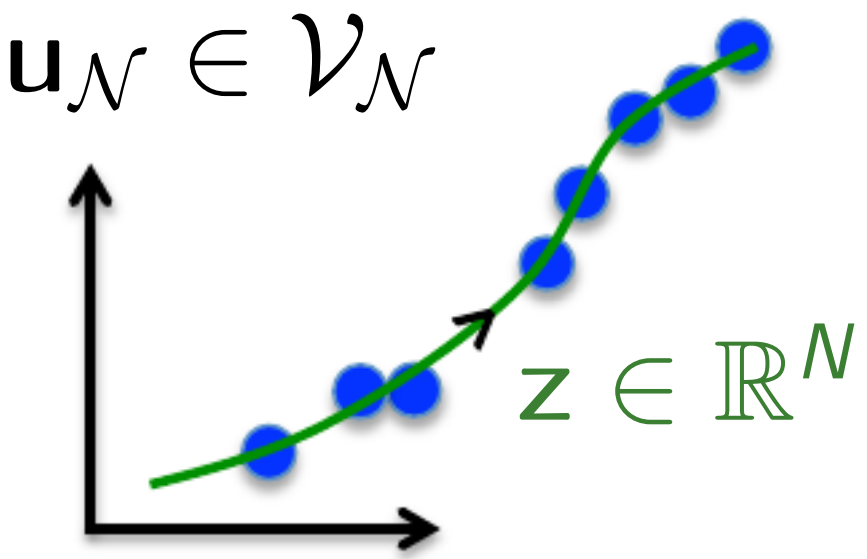

Dimensionality reduction $N < \mathcal{N}$

We expect the simulation data to reveal the computational complexity to use for the reduced order model.

Learning a vector subspace by using the proper-orthogonal decomposition [Lumley 1967]

Proper orthogonal decomosition :

$$\mathbf{u}_{\mathcal{N}}(\mathbf{x},\cdot) \approx \sum_{k=1}^{N} \psi_k(\mathbf{x})\, z_k$$

The proper orthogonal decomposition generalizes the principal component analysis to fields.

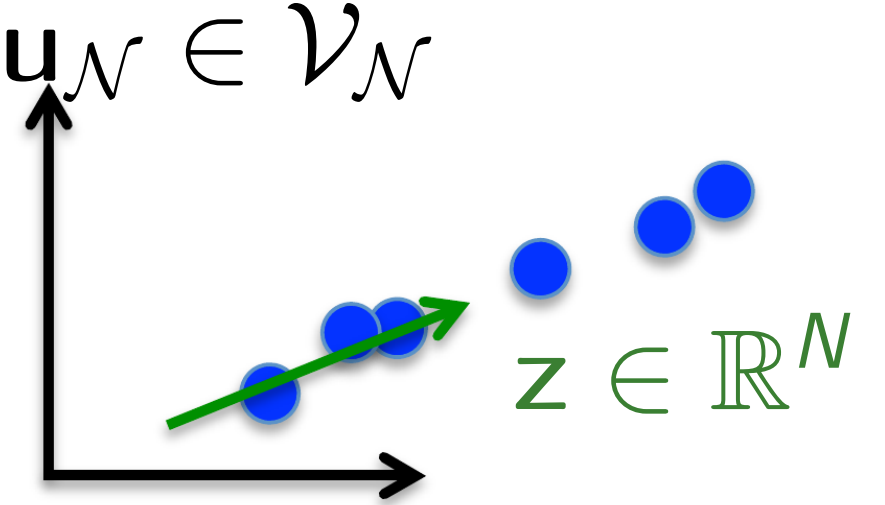

$$\psi_k = \text{argmax}_{\mathbf{v}\in\mathcal{V}_{\mathcal{N}}} \sum_{(t_j,\mu_p)\in\mathcal{D}} \frac{<\mathbf{v},\mathbf{u}_{\mathcal{N}}(\cdot,t_j,\mu_p)>^2}{<\mathbf{v},\mathbf{v}>^2}$$

Reduced basis in $\mathcal{V}_{\mathcal{N}} = \text{span}(\varphi_i)_{i=1}^{\mathcal{N}}$:

$$\psi_k(\mathbf{x}) = \sum_{i=1}^{\mathcal{N}} \varphi_i(\mathbf{x})\, V_{ik}, \qquad \mathbf{V} \in \mathbb{R}^{\mathcal{N}\times N}$$

Projection-Based Model Order Reduction [Aubry, Holmes, Lumley, Stone 1988]

fast reduced predictions of $\mathbf{z}$, $\mathbf{u}_N(\mathbf{x},\cdot) = \sum_{k=1}^{N} \psi_k(\mathbf{x}) z_k$

Galerkin projection reads (from Céa's lemma) :

$$\mathbf{V}^T\, \mathbf{r}(\mathbf{V}\,\mathbf{z}) = 0$$

where $\mathbf{r} \in \mathbb{R}^{\mathcal{N}}$ is the residual of finite element equations [3].

Hyper-reduction via a reduced integration domain Ω_N [Ryckelynck 2005] :

$$\Omega_N = \cup_{i\in\mathcal{F}} \text{supp}(\varphi_i), \qquad \|\mathcal{F}\|_0 \geq N$$

$$\mathbf{V}[\mathcal{F},:]^T\, \mathbf{r}[\mathcal{F}](\mathbf{V}\,\mathbf{z}) = 0$$

Computational complexity of hyper-reduction versus FEM :

Linear solver + γ Constitutive eq. $\qquad (N^3 + \gamma\,\|\mathcal{F}\|_0)/(\mathcal{N}\log(\mathcal{N}) + \gamma\,\mathcal{N})$

3. $r_i = \int_\Omega \varphi_i \,\text{div}\boldsymbol{\sigma}\, d\Omega$

Oblique projection of the high fidelity prediction, in linear elasticity

High fidelity prediction, in linear elasticity :

$$\mathbf{r}(\mathbf{q}) = \mathbf{K}\,\mathbf{q} - \mathbf{F}$$

$$\mathbf{K}\,\mathbf{q} = \mathbf{F}$$

Oblique projection :

$$\mathbf{\Pi}^T := \mathbf{V}[\mathcal{F},:]^T\,\mathbf{K}[\mathcal{F},:]$$

$$\mathbf{q}^{HR} = \mathbf{V}\,(\mathbf{\Pi}^T\,\mathbf{V})^{-1}\mathbf{\Pi}^T\,\mathbf{q}$$

(Gappy POD [Everson 1995] reads : $\mathbf{V}\,(\mathbf{V}[\mathcal{F},:]^T\,\mathbf{V}[\mathcal{F},:])^{-1}\,\mathbf{V}[\mathcal{F},:]^T\,\mathbf{q}[\mathcal{F}]$)

Proof :
$\mathbf{\Pi}^T\,\mathbf{q} = \mathbf{V}[\mathcal{F},:]^T\,\mathbf{K}[\mathcal{F},:]\,\mathbf{q} = \mathbf{V}[\mathcal{F},:]^T\,\mathbf{F}[\mathcal{F}]$, $\mathbf{K}^{HR} = \mathbf{\Pi}^T\,\mathbf{V}$

Convergence in linear elasticity

Exact reduced order basis :

$$\mathbf{q} = \mathbf{V}^{\circ}\, \boldsymbol{\gamma}^{\circ}$$

Convergence depends on the principal angles between $\mathbf{V}^{\circ}$ and $\mathbf{V}$:

$$\|\boldsymbol{\Pi}^{T}\,(\mathbf{q} - \mathbf{V}\,\boldsymbol{\gamma})\|_2 \leq \alpha \sin(\boldsymbol{\theta}(\mathbf{V}^{\circ}, \mathbf{V}))\, \|\boldsymbol{\gamma}^{\circ}\|_2$$

Where $\|\boldsymbol{\Pi}^{T}\, \cdot\, \|_2$ is a truncated error indicator restrained to the RID.

Metrics on vector-bundle manifolds

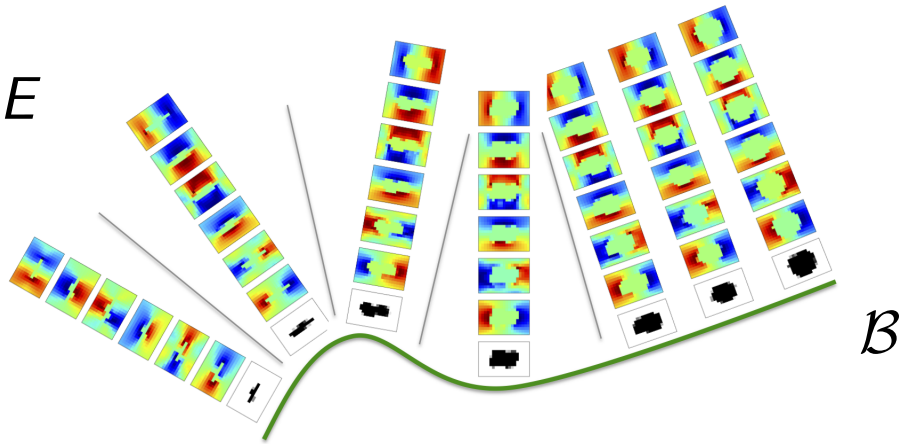

D. Ryckelynck, Th. Goessel, Franck Nguyen. Mechanical dissimilarity of defects in welded joints via Grassmann manifold and machine learning. Comptes Rendus Mécanique, Elsevier, 2020, 348 (10-11), pp.911-935.

Linear manifold :
$\theta < \epsilon$ for $N < 30$.

● ● : Representative data selected via k-medoids (k=2)

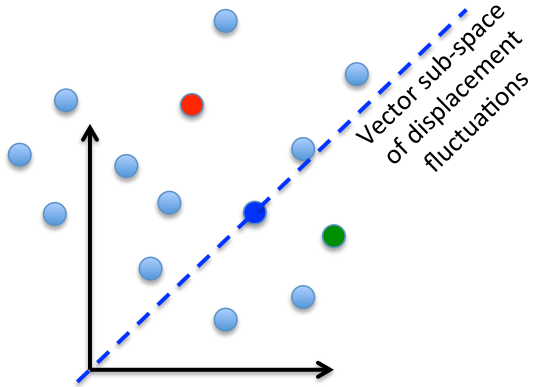

(a): Original Ambient Space

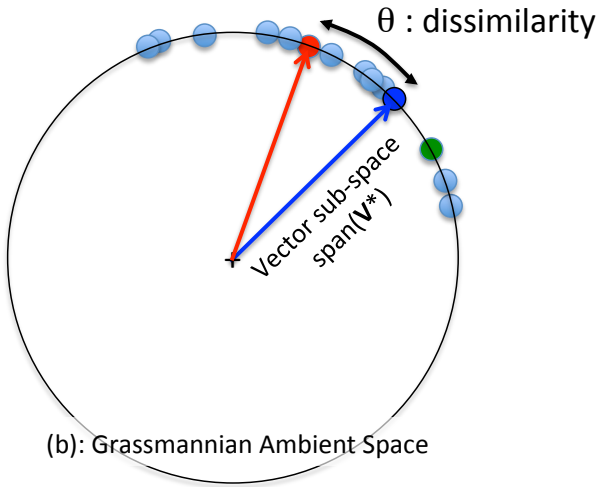

(b): Grassmannian Ambient Space

Numerical example : model calibration in crystal plasticity

Crystal plasticity of Inconel 718 $n = 12$ octahedral FCC slip systems :

$$\dot{\varepsilon}^p = \sum_{s=1}^{n} \dot{\gamma}^s \, \mathbf{m}^s$$

Resolved shear stress :

$$\tau^s = \boldsymbol{\sigma} : \mathbf{m}^s$$

Yield criterion [Meric Cailletaud 1991] :

$$f^s = |\tau^s - x^s| - r^s$$

Rate-independant flow rule [Forest Rubin 2016] :

$$\dot{\gamma}^s = \dot{\varepsilon} \left\langle \frac{f^s}{K} \right\rangle \text{sign}(\tau^s - x^s), \qquad \dot{x}^s = C\dot{\gamma}^s - D|\dot{\gamma}^s|x^s$$

$$\dot{\varepsilon}^2 = \frac{2}{3}(\dot{\boldsymbol{\varepsilon}} - \frac{1}{3}(\mathbf{I} : \dot{\boldsymbol{\varepsilon}})\mathbf{I}) : (\dot{\boldsymbol{\varepsilon}} - \frac{1}{3}(\mathbf{I} : \dot{\boldsymbol{\varepsilon}})\mathbf{I})$$

Parameter ranges

A representative volume of 100 grains may enough for model calibration using macroscopic data [Barbe 2001]. Here, 1000 grains enable more local statistics [Farooq 2019].

$\boldsymbol{\mu}$	Parameter set LK	Parameter set HK
Cubic elasticity	C1111 = 259600 MPa	259600 MPa
	C1122 = 179000 MPa	179000 MPa
	C1212 = 109600 MPa	109600 MPa
Critical res. sh. stress	r^s = 320 MPa	100 MPa
Kinematic hardening	C = 100000 MPa	320000 MPa
	D = 1000	1000
Overstress	K = 9 MPa	9 MPa

Training set using Low Kinematic (HK) hardening, up to 1% of macroscopic strain in a traction test. $\mathcal{D} = \{\boldsymbol{\mu}_{HK}\}$

Testing set using High Kinematic (LK) hardening, up to 0.8% of macroscopic strain.

Macroscopic predictions in case of extrapolation : $\mu \notin \mathcal{D}$

$\mathcal{N} > 3.10^6$, 10 cycles, $N = 10$ (reduced dimension of the latent space).

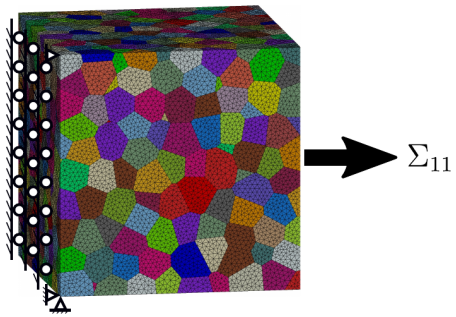

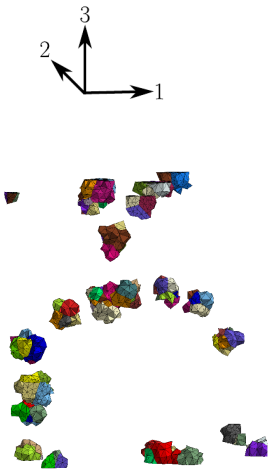

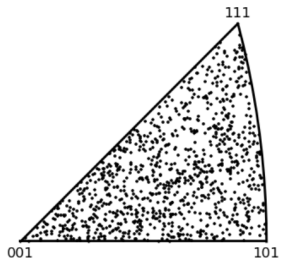

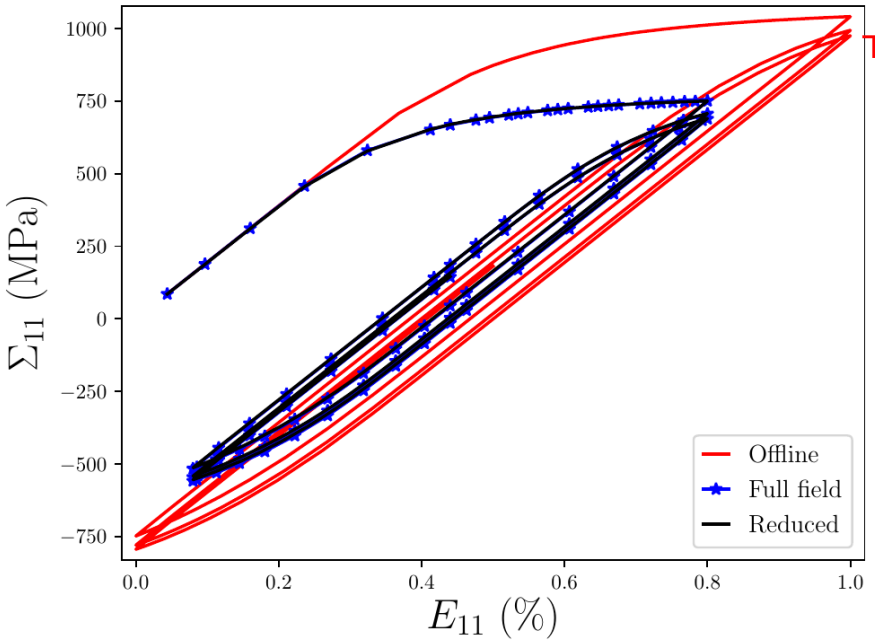

Training data over Ω

Speedup (computational time $\times$ processors) :
$(800\text{h} \times 24)/(70\text{h} \times 1) = 270$

More results using hyper-reduction of cyclic loadings

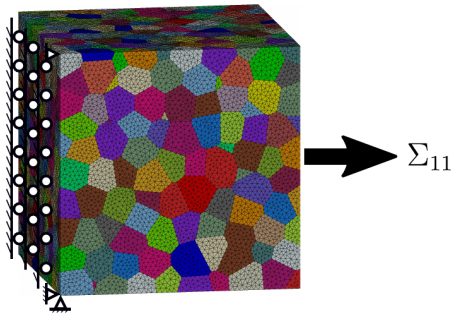

$\mathcal{D}$: train set using 10 loading cycles only.

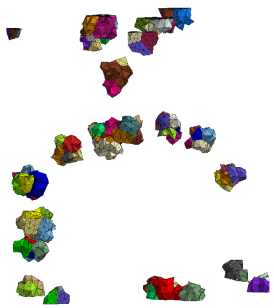

Less than 100 grains in the RID.

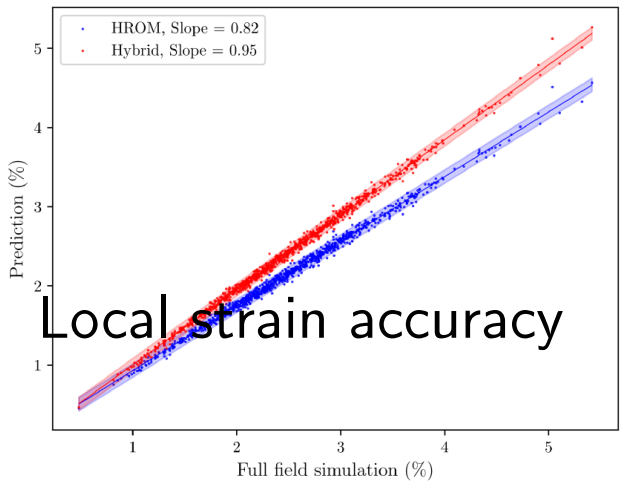

Local strain accuracy

Stress relaxation (under cyclic strain)

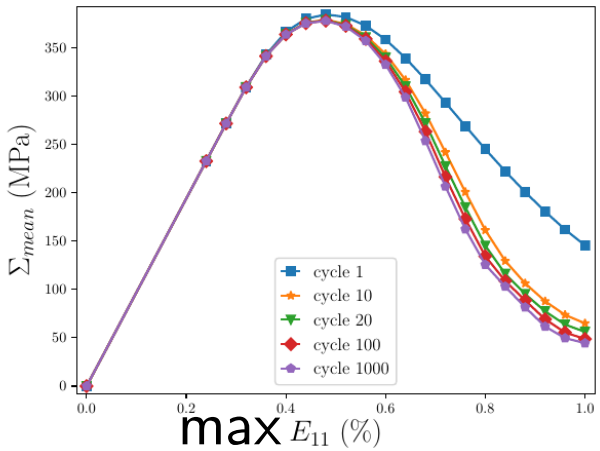

Error estimation on hyper-reduction in plasticity [Ryckelynck 2015]

In case of generalized standard materials, an incremental potential is available :

$$\boldsymbol{\sigma} = \frac{\partial w_\Delta}{\partial \boldsymbol{\varepsilon}}(\boldsymbol{\varepsilon}(\mathbf{u}_N); \boldsymbol{\alpha}_{HR}, \boldsymbol{\mu})$$

where w_Δ is a convex incremental potential with respect to $\boldsymbol{\varepsilon}$ [Ortiz, Suquet, Miehe,...], and $\boldsymbol{\alpha}_{HR}$ are internal variables predicted by the hyper-reduced model.

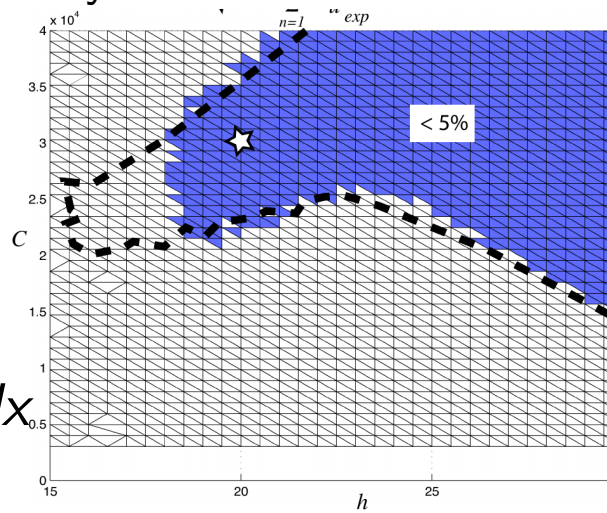

Error indicator

using an admissible stress $\widehat{\boldsymbol{\sigma}}$ (Gappy POD)

$$\eta(\mathbf{u}_N, \widehat{\boldsymbol{\sigma}}) = \sum_{n=1}^{m} \int_\Omega w_\Delta(\boldsymbol{\varepsilon}(\mathbf{u}_N)) + w_\Delta^\star(\widehat{\boldsymbol{\sigma}}) - \boldsymbol{\varepsilon}(\mathbf{u}_N) : \widehat{\boldsymbol{\sigma}}\, dx$$

$$w_\Delta^\star(\widetilde{\boldsymbol{\sigma}}) = \mathrm{Sup}_{\boldsymbol{\varepsilon}^\star}\left(\boldsymbol{\varepsilon}^\star : \widetilde{\boldsymbol{\sigma}} - w_\Delta(\boldsymbol{\varepsilon}^\star)\right), \quad \forall \widetilde{\boldsymbol{\sigma}}$$

Computational complexity of projection-based model order reduction on vector subspaces

Finite Element Models have sparce matrix forms. Their computational complexity that range between $O(\mathcal{N})$ and $O(\mathcal{N}\log(\mathcal{N}))$.

Projection-based reduced order models have dense matrices. Their computational complexity is $O(N^3)$.

In practice, a reduced dimension $N > 30$ is huge when $\mathcal{N} \approx 10^6$.

Contents

About data visualisation

Manifold-learning for data visualization is very popular (i.e. Multidimensional scaling, t-SNE), but here we need equations for latent space in projection-based model order reduction.

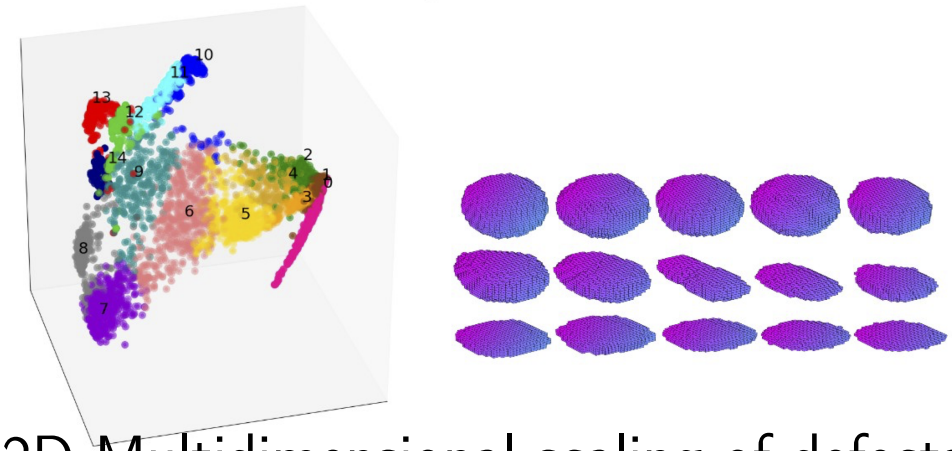

2D Multidimensional scaling of defects in welding joints [Launay 2021]

Auto-encoders for projection-based model order reduction

To retain some meaningful properties of the original data : $\mathbf{y} \approx \mathbf{x}$ (not $=$, for denoising) [Le Cun 1987]

Encoder : $\mathbf{z} = \mathbf{e}(\mathbf{x})$

Decoder : $\mathbf{y} = \mathbf{d}(\mathbf{z})$

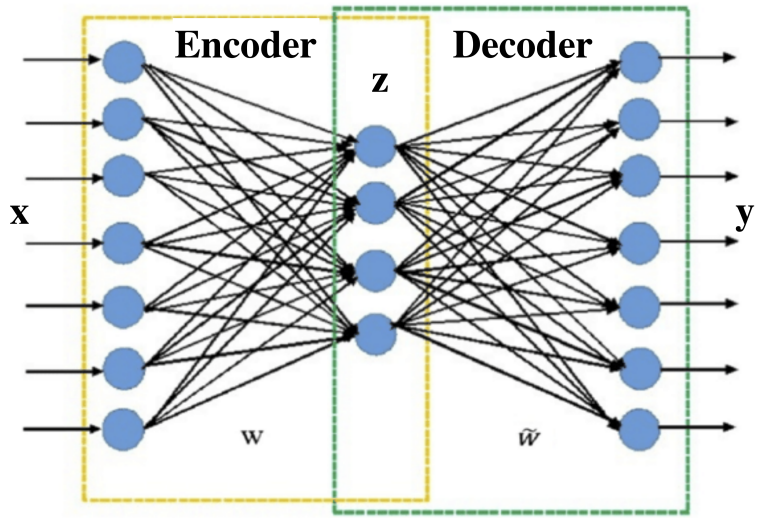

Projection-based model order reduction using autoencoders [Kashima 2016] [a] : for a given $\boldsymbol{\mu}_\square \in \mathcal{D}$ find $\mathbf{z}$,

$$\mathbf{z}(\boldsymbol{\mu}_\square) = \arg \min_{\mathbf{z}^\star \in \mathbb{R}^N} \|\mathbf{r}(\mathbf{d}(\mathbf{z}^\star); \boldsymbol{\mu}_\square)\|, \quad \mathbf{u}_N = \sum_{i=1}^{\mathcal{N}} \varphi_i \, d_i(\mathbf{z})$$

a. 10.1109/CDC.2016.7799153

Piecewise linear approximation of nonlinear manifolds

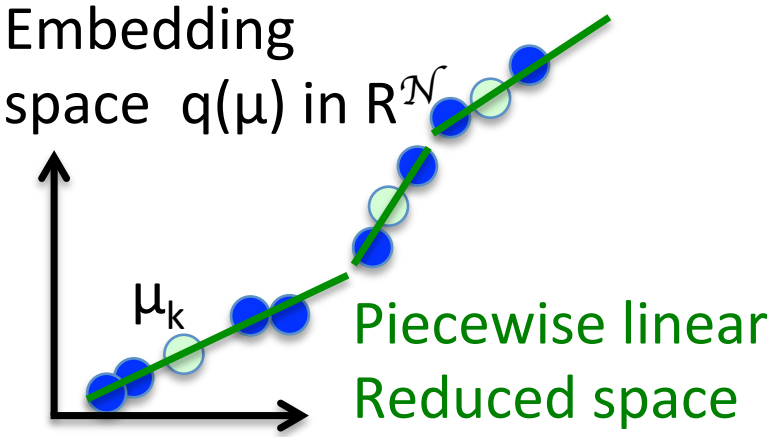

Nonlinear model order reduction based on local reduced-order bases [Amsallem et al. 2012] [a]
Localized Discrete Empirical Interpolation Method [Peherstorfer et al. 2014] [b]

---

a. https ://doi.org/10.1002/nme.4371
b. https ://dspace.mit.edu/handle/1721.1/88242

ROM-net : data clustering aiming at training local reduced order models for image-based modeling and model classification

ROM-net for Uncertainty Quantification in thermomechanics of turbine blades (AM1 superalloy)

$\mu_\square$ = temperature field [Daniel 2020]

https ://doi.org/10.1186/s40323-020-00153-6

$\mathcal{N} = 200000,\ N = 2$

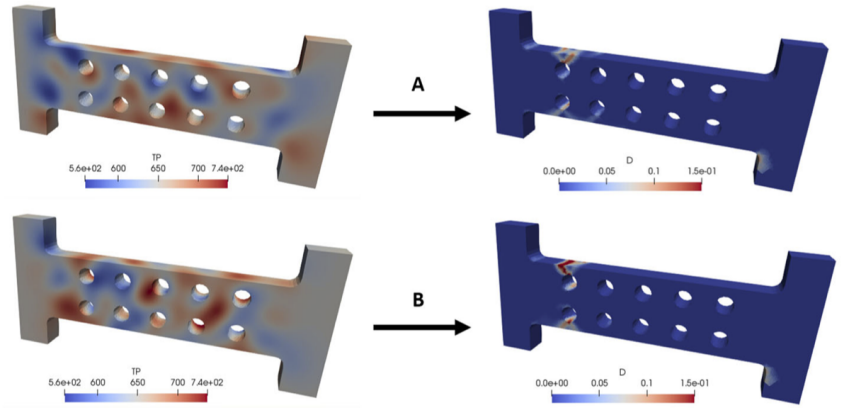

Fig. 6 Influence of the temperature field. Two damage fields (on the right) obtained from two different temperature fields (on the left)

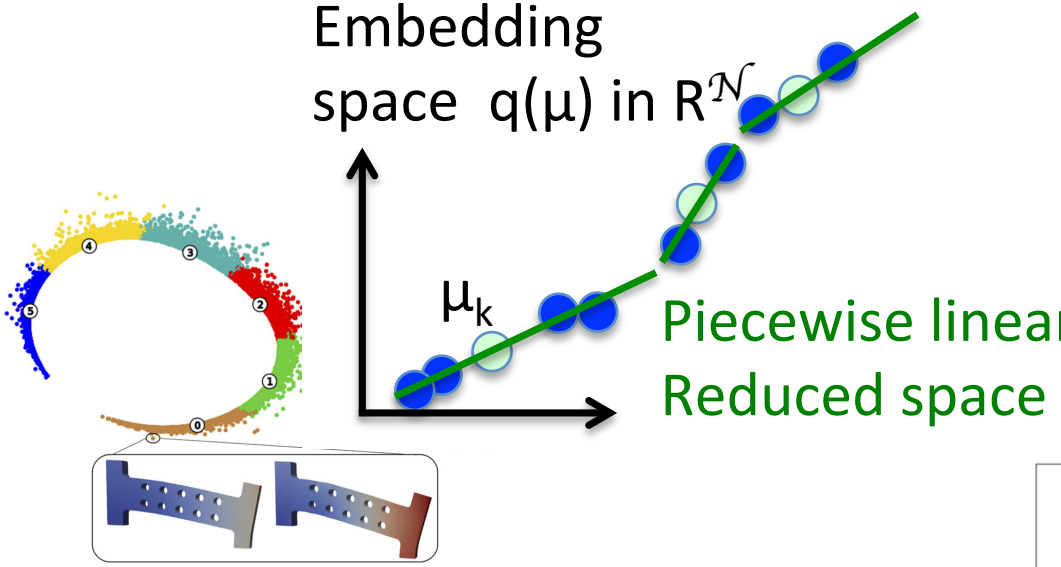

Fig. 7 MDS plots of clustering results. The positions of the clusters' labels correspond to the medoids. Each point corresponds to a subspace $\mathcal{V}(T_i)$ spanned by two displacements fields of the simplified mechanical problem with the thermal loading T_i

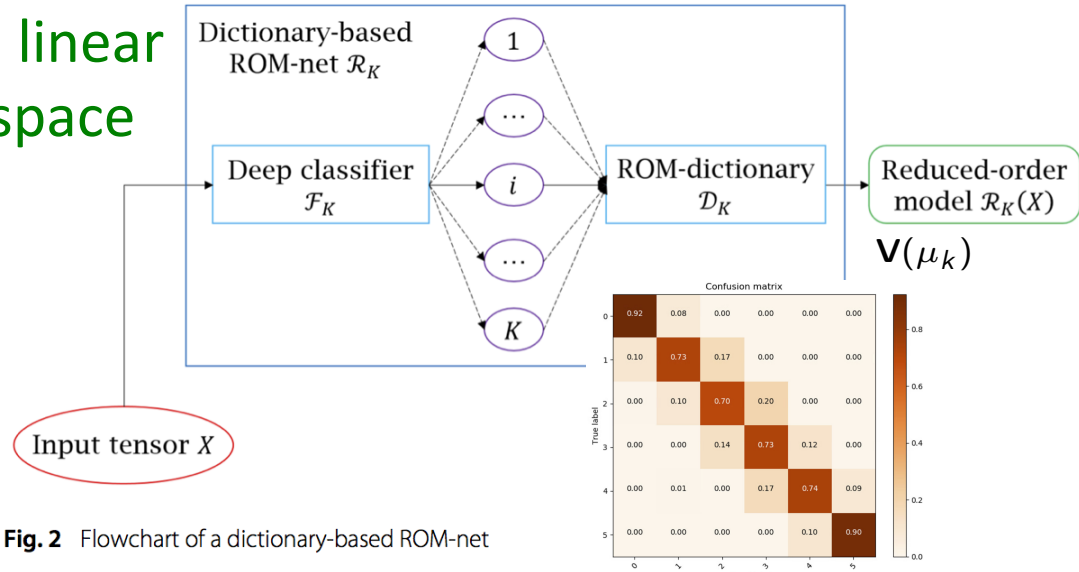

Fig. 2 Flowchart of a dictionary-based ROM-net

Simulation speedup = 60

Error ≈ 5%

Data augmentation for ROM-nets

In a vector bundle, where is the closest neighbor in the base manifold of available digital twins (red points) ?

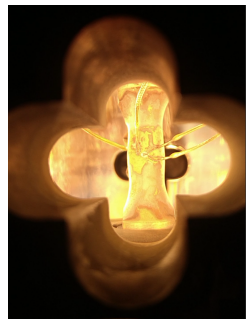

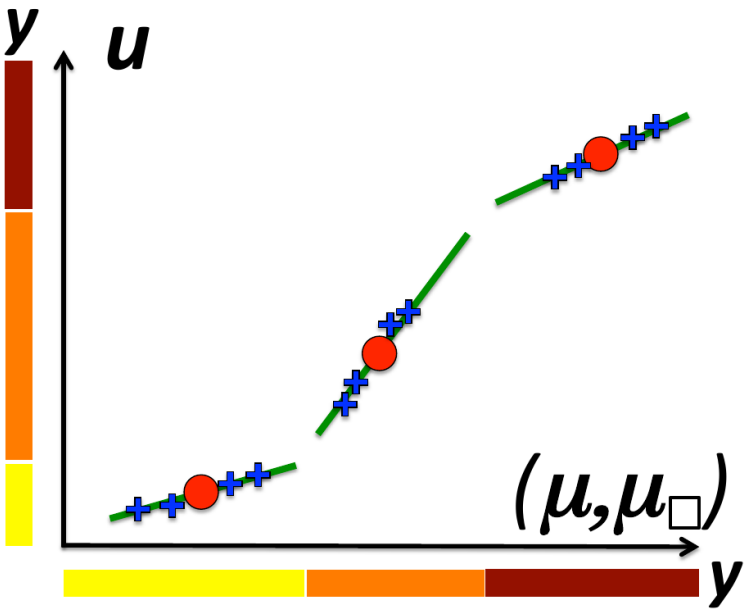

Data augmention schemes have been proposed to train robust classifiers for synthetic data following PDEs.

Multimodal data augmentation for digital twining assisted by artificial intelligence in mechanics of materials, Axel Aublet, Franck N'Guyen, Henry Proudhon, David Ryckelynck, Frontiers, (2022).

Manifold learning for multimodal data

Training set of data : multi-modal data $(\mathbf{d}, \mathbf{u})$, observational and simulation data are assumed to be strongly correlated.

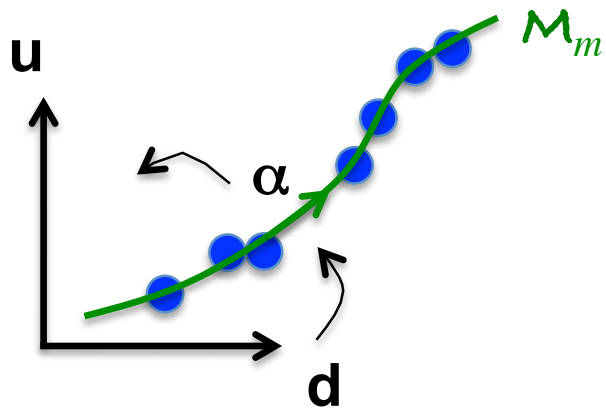

We develop multi-modal latent spaces, $\mathcal{M}_m$, that involve the solution space $\mathcal{M}_u$:

$$(\widetilde{\mathbf{d}}(\boldsymbol{\alpha}),\ \widetilde{\mathbf{u}}(\boldsymbol{\alpha})_{\in \mathcal{M}_u}) \quad \in \mathcal{M}_m$$

where $\boldsymbol{\alpha} = e^d(\mathbf{d})$ is a latent variable of reduced dimension.

Manifold learning using multimodal autoencoders [Launay 2021] [4]

- Add loss function to penalize uncommon representations in the latent space
- Common representation in L_{tot}
- Cross modal reconstruction with one channel
- Representation in latent space

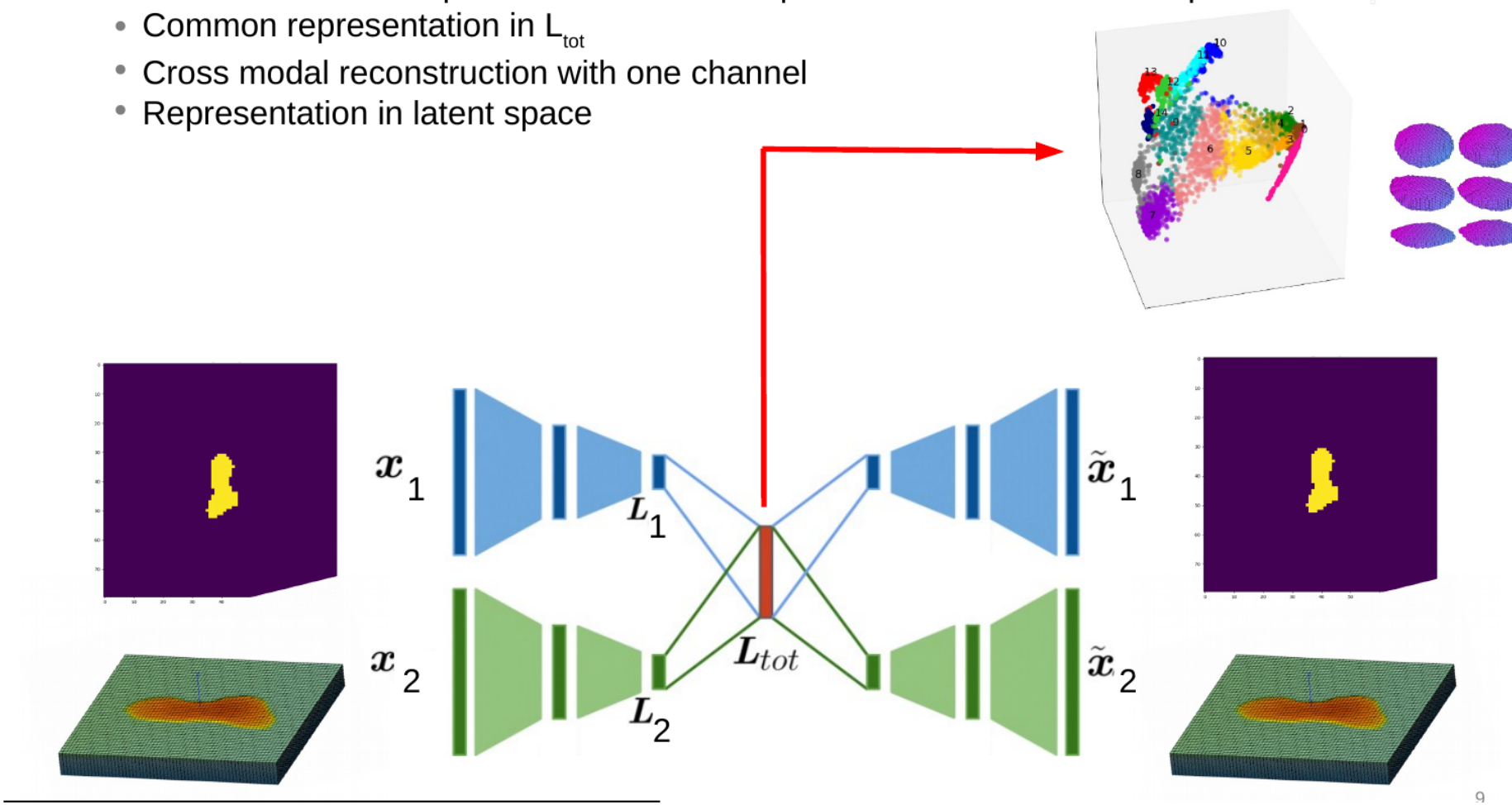

4. Hugo Launay, David Ryckelynck, Laurent Lacourt, Jacques Besson, Arnaud Mondon, et al.. Deep multimodal autoencoder for crack criticality assessment. International Journal for Numerical Methods in Engineering, Wiley, 2021, 123 (6), pp.1456-1480.

Contents

Conclusion

- Vector bundles are relevant for manifold learning applied to digital twining
- The generalisation of a manifold, or its validity domain, is an issue
- Hyper-reduction of local ROM is easy, when introducing a reduced mesh and a modified linear solver.
- Applications :
  - Polycrystalline multimodal datasets (DCT, EBSD, crystal plasticity)
  - Automate process from data acquisition to simulation
  - Model calibration
  - Uncertainty quantification for image-based modeling
  - Health monitoring, inspection assisted by AI, anomaly detection...
  - Margin reduction...

Outlook

Toward a posteriori interpretability using error estimation (for instance) and multi-steps modeling producing intermediate results.

More transfer learning and adaptive learning ...

What is an anomaly in spatialy structured data ? For instance in polycristalline aggregates.

What kind of nonpramateric modeling for morphological uncertainties in polycristalline aggregates ?

Manifold for geometrical variations

Boundaries modes in Ω_K

- Ω_K is observed by X-Ray Diffraction Contrast Tomography.
- This volume contains Γ (assumed grain boundary).
- The Laplace Beltrami eigenmodes ϕ enable "vibrations" in Ω_K :

$$\Delta\phi_k = -\frac{1}{\lambda_k^2}\,\phi_k \quad \text{in } \Omega_K$$

$$\phi_k = 0 \quad \text{in } \partial\Omega_K$$